



## Growth and Crystallization of Titanium Oxide Films at Different Anodization Modes

Jun-Heng Xing, Zheng-Bin Xia,<sup>†</sup> Jian-Feng Hu, Yan-Hong Zhang, and Li Zhong

School of Chemistry and Chemical Engineering, South China University of Technology, Guangzhou, Guangdong 510640, China

The growth process and crystallizing mechanisms of anodic oxide films on highly pure titanium plates are studied in 0.1 M H<sub>2</sub>SO<sub>4</sub> solution at potentiostatic, potential-sweep and combined anodization modes with the same final voltage of 30 V. The influences of anodization mode on the crystalline behavior, surface morphology, chemical composition and electrochemical properties of titanium anodized films are studied. The results show that the potentiostatically grown film is thicker, rougher and more crystalline than the film formed at potential-sweep and combined modes. The titanium oxide film contains an outer porous layer and an inner barrier layer, and the barrier layer of the slow-grown film is much thicker than that of the fast-grown film. For titanium oxide film formed in the potentiostatic mode, "flower-like" crystalline grains are developed due to very high local current density at the local defect sites of titanium surface. In the case of potential-sweep and combined anodization modes, the crystallization of titanium oxide film is homogeneous, which is mainly caused by the internal compressive stresses.

© 2013 The Electrochemical Society. [DOI: 10.1149/2.070306jes] All rights reserved.

Manuscript submitted February 4, 2013; revised manuscript received March 14, 2013. Published March 22, 2013.

Anodic titanium oxide films are of great scientific interest due to their potential use in corrosion protections,<sup>1</sup> solar cells,<sup>2</sup> sensors,<sup>3</sup> batteries,<sup>4</sup> photocatalytic engineering<sup>5,6</sup> and biomedical engineering,<sup>7,8</sup> etc. It is reported that the applicable properties of titanium oxide films are determined by their structure and surface features,<sup>9,10</sup> and the crystalline behavior, chemical composition, surface morphology and electrochemical properties of titanium anodized films are largely dependent on their preparation modes.<sup>11</sup>

For the growth of titanium oxide films, there are mainly three anodization modes, i.e. potentiostatic mode, galvanostatic mode and potentiodynamic mode, and sometimes the combination of these modes is also used. It has been reported that the fast-grown (potentiostatic) anodic oxide layers tend to be thicker and more crystalline than that of the slow-grown (galvanostatic or potentiodynamic) ones.<sup>11–15</sup> By performing titanium anodization both at potentiostatic and potentiodynamic modes, Kudelka et al.<sup>14</sup> revealed that the fast-grown films were thicker and more insulating than the slow-grown films, and the properties of the former were less dependent of the orientation of titanium substrate than that of the latter. Generally speaking, under potentiostatic conditions, the current density at the very beginning stage of anodizing process is usually very large, as a result, many micro-crystals randomly emerge in milliseconds, and then thick and rugged oxide films quickly form on titanium surface. By contrast, in the case of galvanostatic or potentiodynamic modes, titanium oxide films grow with a relatively low rate, and clusters of the TiO<sub>2</sub> crystals are more likely formed.<sup>11</sup>

Moreover, the crystallizing mechanisms of anodic titanium oxides have been also effectively studied with the intent to provide a micro-view for the growth of TiO<sub>2</sub> films at different anodization modes. It is revealed that the crystallization of anodic titanium oxide films is mainly due to two reasons: the local heating and the internal compressive stresses.<sup>16–18</sup> On the one hand, the crystallization of anodic oxides on titanium is considered to be a thermally-induced, slow evolving process, and promoted by enhancing the oxidation potential (i.e. the current density)<sup>19</sup> or by raising the solution temperature.<sup>20,21</sup> In addition, as reported by Yahalom et al.<sup>16</sup> and Dyer et al.,<sup>22</sup> crystallization is always accompanied by breakdown of amorphous anodic titanium oxide films. Although the relationship between film breakdown and crystallization is still uncertain, a generally accepted explanation is that the breakdown can enhance the local current density of anodic oxide film, and thus, crystallization is promoted as a result of local current density or local heating.

On the other hand, the thermally-induced mechanism for the anodic titanium oxide crystallization fails to explain some experimental phenomena. For example, as reported by some authors,<sup>18,23</sup> the TiO<sub>2</sub>

crystals firstly appear at the metal/oxide interface, where no breakdown has occurred and no local high temperature has been produced. This means that titanium oxide crystallization can be induced without local heating. Hence the internal compressive stresses, another cause of titanium anodic oxide crystallization, has been more and more cited in the literatures.<sup>20,24,25</sup> As summarized by Leach et al.,<sup>18</sup> the crystalline films usually occupy smaller volumes as compared with the same weight of amorphous ones, which means that the formation of crystalline structures will be favored with the generation of internal stresses. The compressive stresses are produced at the metal/oxide interface, influenced by the ionic transport numbers. The Pilling-Bedworth ratio (PBR), which is defined as the ratio of the respective volume of the oxide formed and the metal consumed, is the most acceptable source of the generation of internal stresses.<sup>18,26</sup> For amorphous titanium oxides, the PBR is reported as 2.3–2.4,<sup>18</sup> hence it is not surprising that the anodic titanium oxide films will grow with large compressive stresses. Another well established source of compressive stresses is the electrostriction pressure. During titanium anodizing process, the electric field is usually very large (with the order of 10<sup>6</sup>–10<sup>7</sup> V cm<sup>-1</sup>) due to very thin oxide film. As a result, considerable electrostriction pressure (and then compressive stresses) will be produced.<sup>20,27</sup> Therefore, it is considered that the internal compressive stress is one of the main driving forces for the crystallization of the anodic titanium oxides.

Nevertheless, for the film growth at a given anodization mode, it is still unclear that whether the crystallization of titanium oxides should be attributed to local heating or internal compressive stresses, and few works have been reported. The titanium anodization is actually a very complex process, although the effect of anodization mode on formation and crystallization of titanium oxide films has been studied by some researchers, the influence mechanisms are still not well understood. In the present study, the titanium anodization is carried out in 0.1 M H<sub>2</sub>SO<sub>4</sub> solution at potentiostatic, potentiodynamic (potential-sweep) or combined modes. The structure, morphology, composition and electrochemical properties of titanium oxide films formed under different modes are detected, and the growth process and crystallizing mechanisms of titanium oxide films under different anodization conditions are discussed.

### Experimental

**Sample preparation.**— Highly pure titanium sheets (>99.99%, 1 mm thick) with a size of 10 × 10 mm were used as the working electrode. Prior to anodization, all samples were mechanically polished with 600, 1000, 1500 and finally with 3000 emery papers, and then ultrasonically cleaned for 20 min with acetone and later for 20 min with deionized water. Subsequently, these samples were

<sup>†</sup>E-mail: cezhbxia@scut.edu.cn

chemically polished by etching in a solution of 1% HF and 3% HNO<sub>3</sub> for 3~4 s, and then ultrasonically cleaned for 20 min with deionized water again.

**Anodic oxidation.**— Anodic oxide films of titanium were formed in a two-electrode electrochemical cell, controlled by an Autolab potentiostat-galvanostat device which was equipped with a Voltage Multiplier module (Metrohm PGSTAT100, Switzerland). A platinum sheet was used as the counter electrode. The electrolyte was 0.1 M H<sub>2</sub>SO<sub>4</sub> solution, which was stirred with purified nitrogen gas before and during sample anodization. Three anodization modes, the potentiostatic mode, the potential-sweep mode and the combined mode were used in this study. In the case of potentiostatic mode, constant oxidation voltage of 30 V was maintained for 60 min. For the potential-sweep mode, the potential was swept from 0 to 30 V at a constant sweep rate of 0.01 V/s. For the combined growth mode, the same process as the potential-sweep anodization was first performed, and then the potential was kept at 30 V for 60 min (potential-aging stage). All experiments were carried out at 25 °C. After anodic oxidation, the samples were immediately removed from the solution, rinsed with distilled water, and then dried by air blowing before further characterization.

**Film characterization.**— A Raman spectrometer (HORIBA Jobin Yvon LabRAM Aramis, France), equipped with an optical microscopy (Olympus, Japan), was used to detect the structure of anodic oxide films on titanium. The excitation wavelength was 532 nm, and the incident power was 10.4 mW. Scanning electron microscopy (SEM, LEO 1530 Vp, Germany) with electron beam of 5 kV was used to observe the surface topography of titanium oxide films. Atomic force microscopy (AFM, Benyuan CSPM 4000, China) was used to detect the morphology and surface roughness of the formed TiO<sub>2</sub> films in air by a tapping mode with the cantilever of Tap 300 Al. AFM 3D images were obtained by using the accompanied Image 4.60 software. Spectroscopic ellipsometer (SE, HORIBA Jobin Yvon Auto SE, France), which was performed at an incidence angle of 70° with the wavelength range from 439 nm to 842 nm, was used to determine the thickness of titanium oxide films. In measuring film thickness, a single layer model (Ti substrate and TiO<sub>2</sub> layer) was used in modeling procedure. X-ray photoelectron spectrometry (XPS, Kratos Axis Ultra DLD, UK), us-

ing an Al K $\alpha$  (1486.6 eV) radiation source and operated at 15 kV and 150 W, was used to determine the chemical composition analysis of titanium anodized films. The Shirley background was used for peak fitting, and all spectral positions were corrected by setting the C 1s peak at 284.6 eV.

**EIS.**— Electrochemical impedance spectroscopy (EIS), which was carried out by using an Autolab electrochemical workstation (Metrohm PGSTAT100 with FRA module, Switzerland) in a traditional three-electrode cell, was used to perform the electrochemical characterization of titanium anodized films. A platinum plate was used as the counter electrode, a saturated calomel electrode (SCE) was presented as the reference electrode, and the solution was 50 g/L NaCl. The exposed area of working electrode was 0.5 cm<sup>2</sup>. The specimen was initially immersed in the solution for 0.5 h, and then the EIS measurements were performed under potentiostatic mode at open-circuit potentials with the frequency range of 10<sup>-2</sup> to 10<sup>5</sup> Hz and the amplitude of 10 mV.

## Results and Discussion

**Structure.**— Raman spectroscopy, a powerful tool for characterization of anodic oxide films on titanium, is thought to be an alternative technique for detection of crystalline TiO<sub>2</sub> as compared to the standard X-ray and electron diffraction.<sup>28</sup> Fig. 1a displays the Raman spectra of titanium oxide films formed by different anodization modes. Four Raman bands at about 144 cm<sup>-1</sup>, 399 cm<sup>-1</sup>, 516 cm<sup>-1</sup> and 639 cm<sup>-1</sup>, corresponding to anatase type of TiO<sub>2</sub>, can be clearly found for all samples, indicating that whatever anodization mode is performed, crystalline titanium oxide films can be formed with the final oxidation potential of 30 V.

The optical microscopy photos of the anodized titanium surface under potentiostatic and potential-sweep conditions are shown in Fig. 1b. The surface image of the film grown under combined mode is very close to that of the film grown at potential-sweep mode, hence it is not presented here. The picture of the potentiodynamically grown film shows a relatively flat surface and homogeneous features. The image of the potentiostatically grown film has two distinguishable regions, the black and the white region, which means that the crystallization of the titanium oxide film is nonuniform. These findings are

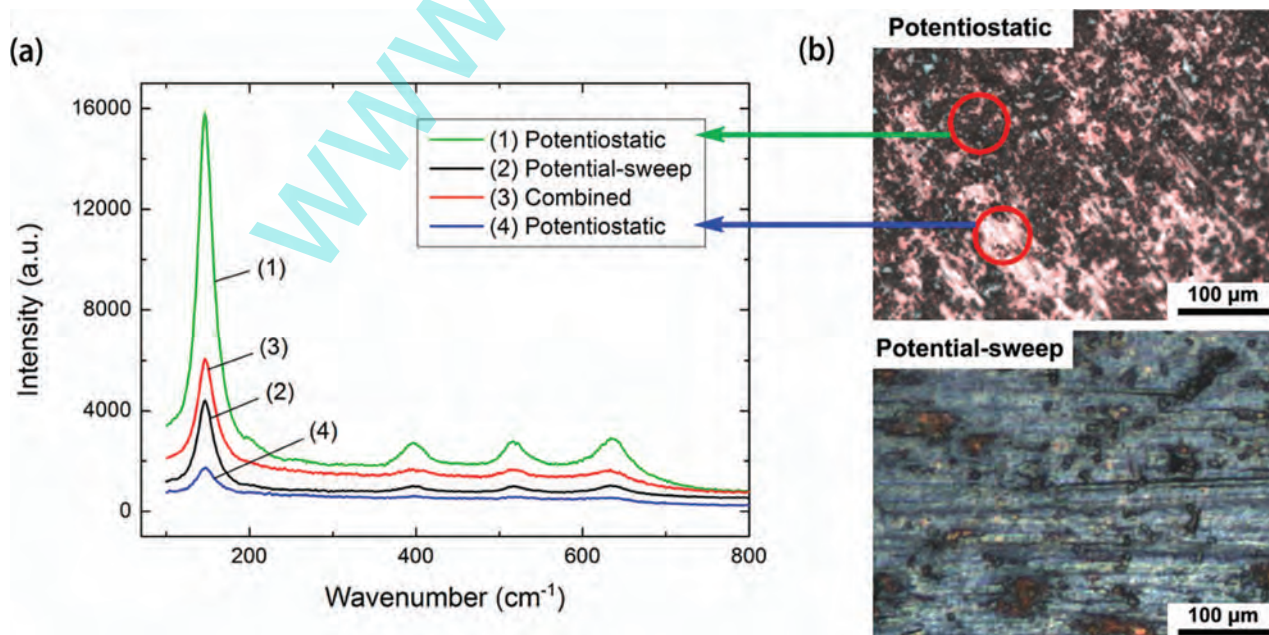


**Figure 1.** (a) Raman spectrum of titanium samples anodically oxidized at different modes and (b) optical microscopy pictures of anodized titanium surface under potentiostatic and potential-sweep conditions.

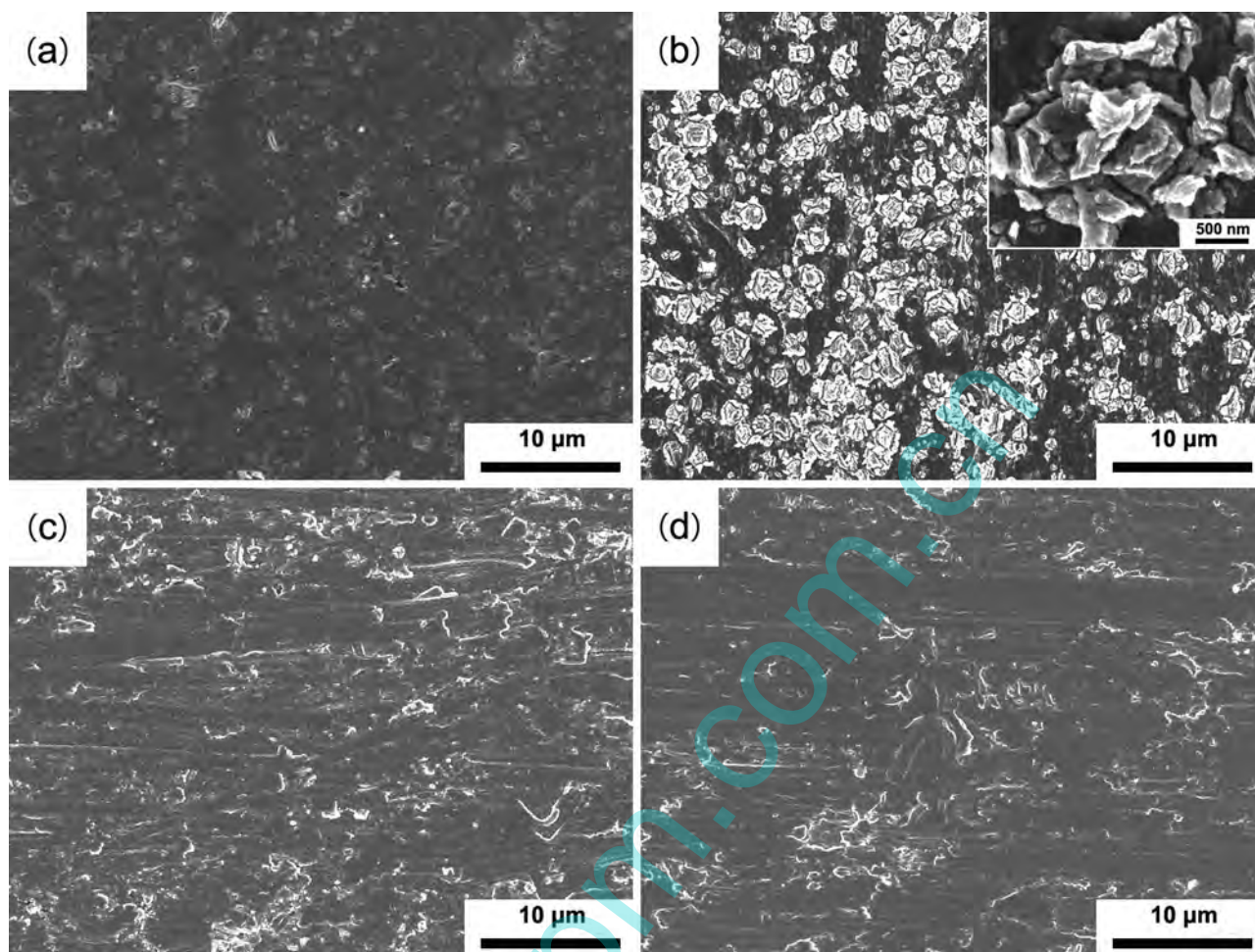


**Figure 2.** SEM images of (a) titanium substrate and anodic titanium oxide films formed by (b) potentiostatic, (c) potential-sweep and (d) combined modes.

also proved by the Raman spectra, which have been recorded from different regions of the titanium oxide film surface more than seven times for each anodized sample.

In the case of the potential-sweep and combined mode, the peak height of the Raman spectrum of the titanium oxide films shows a well reproducibility within an error limit of about 15%, which means that these films are homogeneously crystallized (Fig. 1a, spectrum 2 and 3). By contrast, for the potentiostatically grown film, the Raman spectra recorded from different regions show two distinguishable features. When the Raman microlaser beam is centered respectively on the black and the white region (Fig. 1b, Potentiostatic), the results are shown in the spectrum (1) and (4), respectively, in Fig. 1a. It is clearly that the peak intensity of the spectrum (1) is much higher than that of the spectrum (4), which implies that the black region of the potentiostatically grown film is more crystalline than the white region. In other words, the fast-grown film is heterogeneously crystallized. It should be noted that for the potentiostatically grown oxide film, although the Raman spectrum shows that it has two distinguishable crystallization regions, most of the film surface (about 75%) is related to the spectrum (1) shown in Fig. 1a. From this point of view, it can be considered that the titanium oxide film formed by potentiostatic mode has a more crystalline quality compared to the film formed at potential-sweep and combined modes.

**Surface morphology.**— Fig. 2 shows the SEM images of titanium substrate and anodic titanium oxide films formed by potentiostatic, potential-sweep and combined modes. Similar to the results of Raman spectra, the surface morphology of titanium anodized films formed under different anodization conditions also shows some great differ-

ences. For the potentiostatically grown film, as shown in Fig. 2b, numerous randomly distributed white grains, with a diameter ranging from 0.5 to 2  $\mu\text{m}$ , can be clearly observed. The image inset in the upper right in Fig. 2b shows the magnification of these grains, in which a “flower-like” structure can be clearly seen. According to some authors, these “flower-like” or “nodule-like” structures are composed of crystalline  $\text{TiO}_2$ .<sup>24,29</sup> By contrast, for the oxide films formed at potential-sweep and combined anodization modes (Fig. 2c and 2d), their surface is relatively flat and smooth, and no individual crystalline grains can be distinctly observed, which is very close to the surface morphology of titanium substrate (Fig. 2a).

Fig. 3 presents the AFM 3D images of titanium substrate and titanium anodized films produced under different anodization conditions. As shown in Fig. 3, the AFM images are in good agreement with the SEM results. In the case of potentiostatic mode, randomly distributed  $\text{TiO}_2$  crystalline grains, with the size close to the SEM result, can be clearly observed on the surface of titanium anodized films (Fig. 3b). For the potential-sweep and combined anodization modes (Fig. 3c and 3d), the sample surface is a little rougher than titanium substrate (Fig. 3a), due to the formation of anodic titanium oxides. However, as compared with the potentiostatically grown film, the titanium oxide films formed at potential-sweep and combined modes are much smoother, and almost no distinguishable crystalline grains can be found on their surfaces.

The thickness of anodic titanium oxide films formed by potentiostatic, potential-sweep and combined anodization modes are measured by SE, the average roughness ( $R_a$ ) and the root mean square roughness ( $R_{ms}$ ) of the films surface are calculated from the AFM measurements, and the results are displayed in Table I. It can be found that the

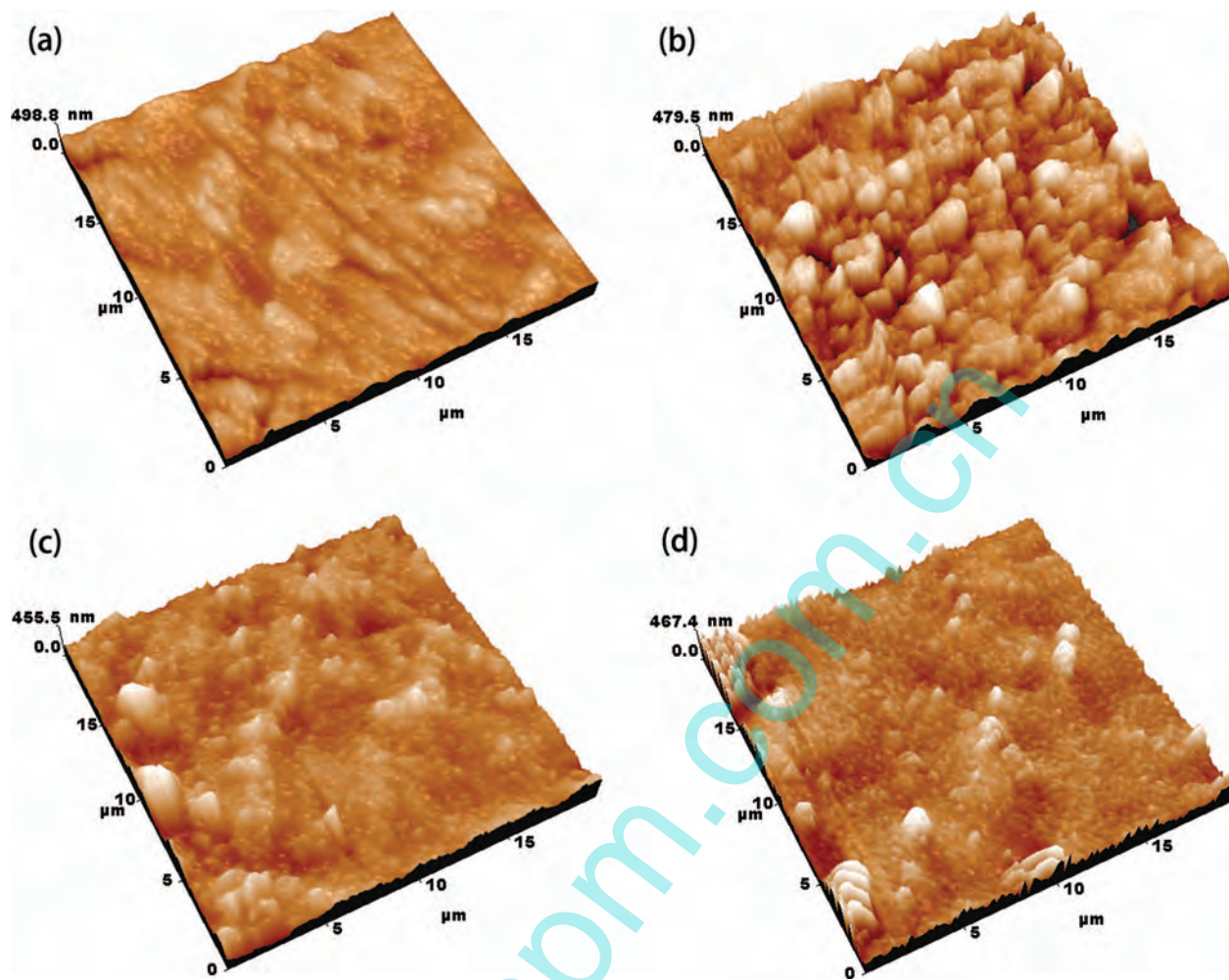


**Figure 3.** AFM 3D images ( $20 \times 20 \mu\text{m}$ ) of (a) titanium substrate and anodic titanium oxide films produced under (b) potentiostatic, (c) potential-sweep and (d) combined conditions.

morphology and thickness of the anodic oxide films depending on their produced conditions: the potentiostatically grown layer is rougher and thicker than the film formed under potential-sweep and combined conditions.

Comparing the films formed at the potential-sweep and the combined anodization modes, it is interesting to find that the film formed at combined mode is only 2.3 nm thicker than the film grown under potential-sweep control, and their surface roughness is also very close to each other. In addition, according to Fig. 1a, the Raman bands intensity of the film grown at combined mode is also only a little higher than that of the potentiodynamically grown film. This means that for the combined mode, the anodic oxide film is mainly formed during the initial potential-sweep process, and the followed potential-aging processing contributes little to the film growth and crystallization.

**Table I. Thickness and surface roughness of titanium substrate and anodic titanium oxide films formed under different anodization modes.**

Anodization modes	$d$ (nm)	$R_a$ (nm)	$R_{ms}$ (nm)
Ti substrate	—	28.1	37.0
Potentiostatic	105.2	52.7	65.3
Potential-sweep	72.8	36.1	46.6
Combined mode	75.1	37.2	47.8

*Chemical composition.*— XPS is a very sensitive characterization method which can provide the chemical composition information of the very top surface of titanium anodized samples. Fig. 4 displays the high resolution narrow Ti 2p and O 1s XPS spectra of anodic titanium oxide films formed at different preparation modes. For all samples, the Ti 2p XPS spectra can be only fitted with 2 peaks which are both attributed to  $\text{Ti}^{4+}$ , indicating that the formed anodic oxide films are mainly composed of  $\text{TiO}_2$  (Fig. 4a). Moreover, the Ti 2p 3/2 peak position of the oxide film grown at potential-sweep and combined modes is about 458.45 eV, very close to the peak location of  $\text{Ti}^{4+}$  reported in the literature (458.42 eV),<sup>12,30</sup> while the Ti 2p spectrum of the potentiostatically grown film clearly shows a weak shift toward lower binding energy (the Ti 2p 3/2 peak position is about 458.31 eV). To the best of our knowledge, this phenomenon may imply that the film formed by potentiostatic control also contains a small amount of titanium suboxides ( $\text{Ti}_2\text{O}_3$  and  $\text{TiO}$ ).<sup>31</sup>

The O 1s XPS spectrum from the formed films can be resolved into 3 peaks, which are attributed to  $\text{O}^{2-}$ ,  $\text{OH}^-$  and  $\text{H}_2\text{O}$ , respectively (Fig. 4b, 4c and 4d). The peak position and the percentage area of the separated peaks from the O 1s spectrum of the anodic titanium oxide films formed at different growth modes are listed in Table II, in which the  $\text{O}^{2-}$  species is mainly from the titanium oxides, the  $\text{OH}^-$  is acted as bound water and the  $\text{H}_2\text{O}$  species may belong to the adsorbed water.<sup>12,20,32</sup> It can be found that the concentration of  $\text{O}^{2-}$  is lower for the potentiostatically grown film than the potentiodynamically grown film, indicating that the potential-sweep condition is beneficial for the dehydration of titanium anodized films. Moreover, by comparing

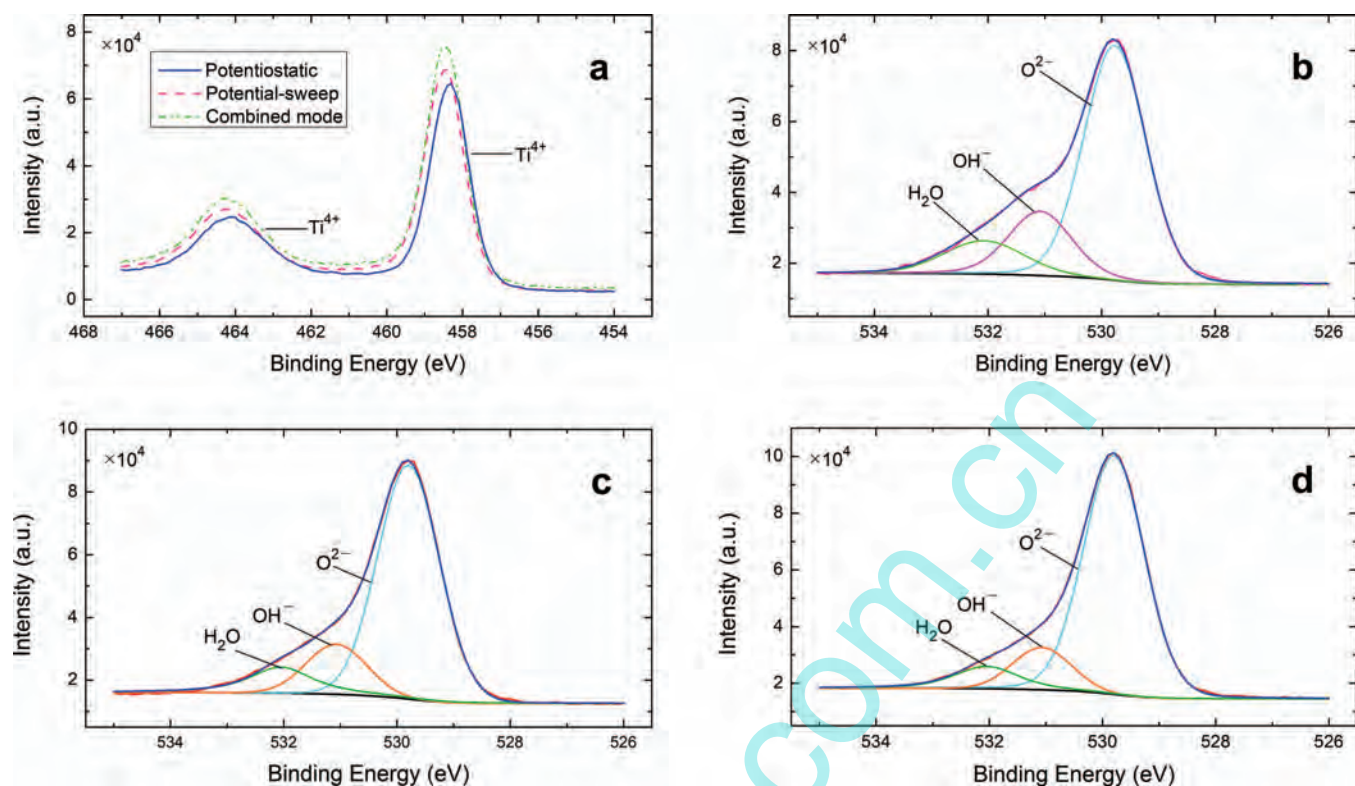


**Figure 4.** (a) Ti 2p XPS spectra of titanium oxide films formed by different anodization modes and O 1s spectra of titanium anodized films grown by (b) potentiostatic, (c) potential-sweep and (d) combined modes.

**Table II.** Peak position and percentage contents of the surface species from O 1s spectrum of titanium anodized films formed at different anodization modes.

Surface species	Binding energy (eV)	Peak area (%)		
		Potentiostatic	Potential-sweep	Combined mode
O <sup>2-</sup>	529.79	68.05	73.34	78.06
OH <sup>-</sup>	531.27	19.63	15.15	12.75
H <sub>2</sub> O	532.07	12.32	11.51	9.19

the anodic titanium oxide films grown under potential-sweep and combined modes, it can be found that the concentration of O<sup>2-</sup> is higher for the film formed under combined mode, which implies that a dehydrated process has been taken place at the potential-aging stage of the combined anodization process.

*EIS.*— Fig. 5 displays electrochemical impedance data of titanium anodized samples in the form of Bode phase plot and Bode impedance plot. The Bode plot of the impedance data for the oxide film formed by the combined mode is similar to that of the potentiodynamically grown film, therefore, it is not presented. The electrochemical data are analyzed by using the equivalent circuit illustrated in Fig. 6, and the fitting curves are also presented in Fig. 5. As shown in the figure, the

simulated curves are in good agreement with the experimental data, indicating that the titanium anodized film contains an outer porous layer and an inner barrier layer. Similar findings were also reported in some other works.<sup>29,33,34</sup>

The equivalent circuit parameters for titanium oxide films grown under different conditions are summarized in Table III. It is shown that the  $R_{pr}$  and  $R_b$  value of the potentiostatically grown film are lower than that of the potentiodynamically grown film. As revealed in Fig. 1, the fast-grown film is more crystalline than the slow-grown film, and the crystallization is proved to produce a path of higher electrical and ionic conductivity than the amorphous oxide,<sup>23</sup> as a result, the potentiostatically grown film will show a lower resistance value than the film formed under potential-sweep control. Moreover, the capacitance ( $C$ ) of the outer layer and the inner layer can be calculated by using Eq. 1 which is proposed by Hsu and Mansfeld:<sup>35</sup>

$$C = Q(\omega_m)^{n-1} \quad [1]$$

in which  $\omega_m$  represents the frequency where the imaginary part of the impedance ( $Z''$ ) reaches its maximum. The  $C$  values of the porous layer and the barrier layer of titanium anodized films grown by different modes are shown in Table IV. For the potentiostatically grown film, the  $C_{pr}$  value are slightly higher and the  $C_b$  value are much higher as compared to the potentiodynamically grown film. We assume the metal/film interface and the film/solution interface as a parallel plate capacitor, and the classic expression of the capacitance of parallel

**Table III.** Equivalent circuit parameters for titanium oxide films formed under different anodization modes.

Anodization modes	$R_s$ ( $\Omega$ )	$R_{pr}$ ( $k\Omega cm^2$ )	$Q_{pr}$ ( $s^n/\Omega cm^2$ )	$n_1$	$R_b$ ( $k\Omega cm^2$ )	$Q_b$ ( $s^n/\Omega cm^2$ )	$n_2$
Potentiostatic	12.15	0.276	$1.806 \times 10^{-5}$	0.9095	28.82	$6.865 \times 10^{-5}$	0.9295
Potential-sweep	10.3	1.463	$1.656 \times 10^{-5}$	0.8385	76.32	$3.92 \times 10^{-6}$	0.9648
Combined mode	11.21	1.257	$1.582 \times 10^{-5}$	0.8542	68.5	$4.51 \times 10^{-6}$	0.9542

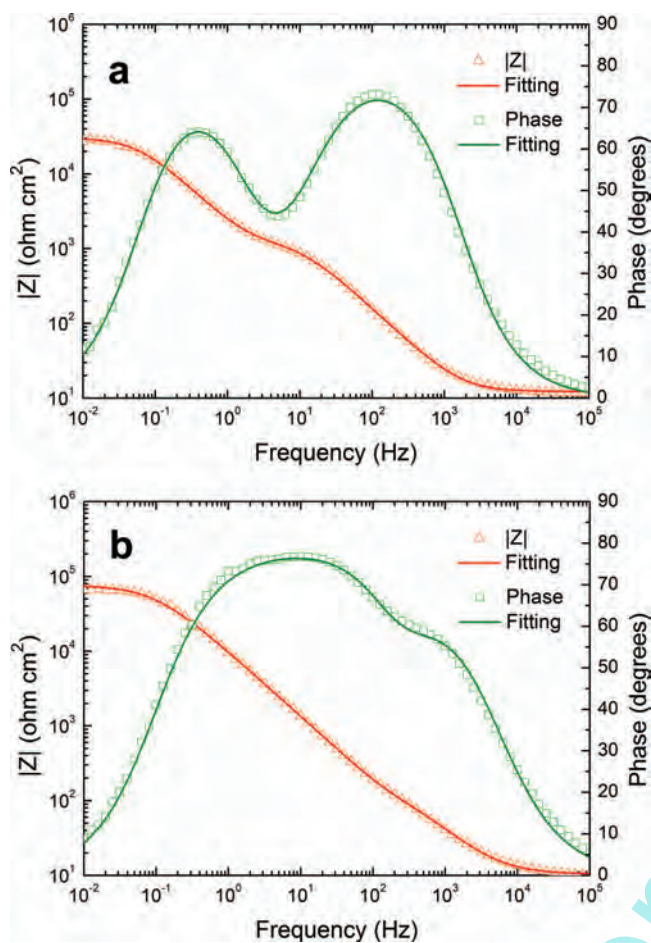


**Figure 5.** Bode plot of impedance data and fitting curves for titanium anodized films grown by (a) potentiostatic and (b) potential-sweep modes.

plate capacitor is shown as below.<sup>21,34</sup>

$$C = \frac{\epsilon_0 \epsilon}{d} \quad [2]$$

where  $\epsilon_0$  is the dielectric constant in vacuum,  $\epsilon$  is the dielectric constant of oxide film and  $d$  represents the layer thickness. Therefore, the capacitance is varied as a function of film dielectric constant and film thickness. For the outer porous film, the value of  $\epsilon$  is largely determined by the film porosity (i.e. the film surface roughness). The film dielectric constant value increases with the film surface roughness, for the reason that the  $\epsilon$  value of the solution is much larger than that of the titanium oxide film.<sup>34</sup> In the case of the inner barrier layer, the film dielectric constant depends on the film crystallinity. Similarly, the  $\epsilon$  value increases with the film crystallinity, because the  $\epsilon$  value of the crystalline oxides is larger than that of the amorphous ones.<sup>21</sup>

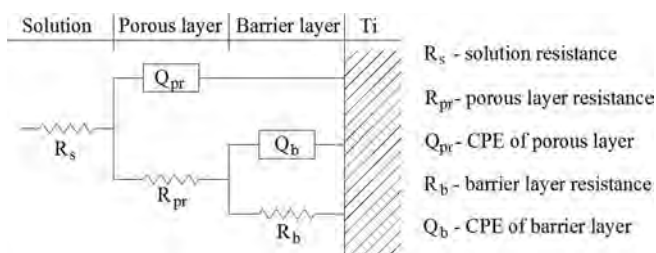


**Figure 6.** Equivalent circuit used for fitting EIS results.

**Table IV.** Capacitance of porous layer and barrier layer and thickness of barrier layer for titanium anodized films formed under different modes.

Anodization modes	$C_{pr}$ ( $\mu\text{F}/\text{cm}^2$ )	$C_b$ ( $\mu\text{F}/\text{cm}^2$ )	$d$ of inner layer (nm)
Potentiostatic	25.63	84.78	0.5
Potential-sweep	24.02	4.25	9.99
Combined mode	22.13	5.01	8.48

For the fast-grown film, the surface roughness is much larger than the slow-grown one (Fig. 2 and Table I), and as seen in Table I, it is not difficult to find that the porous layer thickness of the potentiostatically grown film is larger than that of the potentiodynamically grown film. As a result, the  $C_{pr}$  value of the former is only slightly higher than that of the latter. As for the  $C_b$  value of the inner layer, the crystallinity of the fast-grown film is larger than the slow-grown one, then, the barrier layer of the former will have a higher  $\epsilon$  value. In addition, the barrier layer of the potentiostatically formed oxide film must be much thinner than that of the potentiodynamically grown one, as a result, the  $C_b$  value for the potentiostatically grown film is much larger than the film formed under potential-sweep control. Similarly, for the oxide film grown at combined mode, its film thickness, surface roughness and film crystallinity are all slightly higher than the potentiodynamically grown film (Fig. 1 and Table I), hence its film resistance ( $R_{pr}$  and  $R_b$ ) and  $C_{pr}$  value are slightly lower and its  $C_b$  value is slightly higher than the potential-sweep sample.

By using Eq. 2, we can also calculate the inner layer thickness of titanium anodized films. Because the Raman results show that the crystalline form of the films is anatase, hence the film dielectric constant  $\epsilon$  can be considered as 48.<sup>21</sup> The  $\epsilon_0$  value is  $8.85 \times 10^{-12}$  F/m and the  $C$  values of the inner layer are listed in Table IV. Thickness of the inner layer of titanium oxide films formed at different anodization modes are displayed in Table IV, it is clearly that the barrier layer thickness is much larger for the slow-grown oxide film as compared to the fast-grown one.

**Growth and crystallization of titanium anodized films.**— Fig. 7 shows the evolution of the current density with oxidation time (or voltages) for titanium anodization at different modes. For the potentiostatic mode (Fig. 7a), the current density is initially very large and has a sudden drop at the very beginning stage of anodizing process, which indicates that a passive layer of titanium oxide has been formed in only few seconds. After the initial drop, the current density slightly increases with anodizing time due to the oxygen evolution reaction (OER),<sup>23</sup> which implies that the titanium anodization was in a potential-aging stage. At this stage, the anodic oxide film will grow slowly, accompanied by the conversion of titanium suboxides and hydroxides into titanium dioxides.<sup>30</sup>

In the case of potential-sweep anodization mode (Fig. 7b), the current density starts with about zero and then gradually increases with the anodizing potentials, this means that the growth of titanium oxide film goes through a very slow process. It should be noted that a small peak current at about 10 V maybe due to the OER,<sup>23</sup> and after then, the current increase rate is significantly enhanced as a result of film crystallization. For the combined mode, the evolution of the current density also shows a combined feature: it first increases with the oxidation voltages, and then keeps a constant value in the potential-aging stage.

Taking into account the results mentioned above, the growth process and crystallizing mechanisms of anodic titanium oxide films under different anodization conditions are put forward and shown in Fig. 8.

In the case of potentiostatic mode, numerous micro-crystals are randomly emerged at the beginning of titanium anodization and grow to “flower-like” crystalline grains in the followed potential-aging stage (Fig. 8). In order to well explain this phenomenon, let us first make

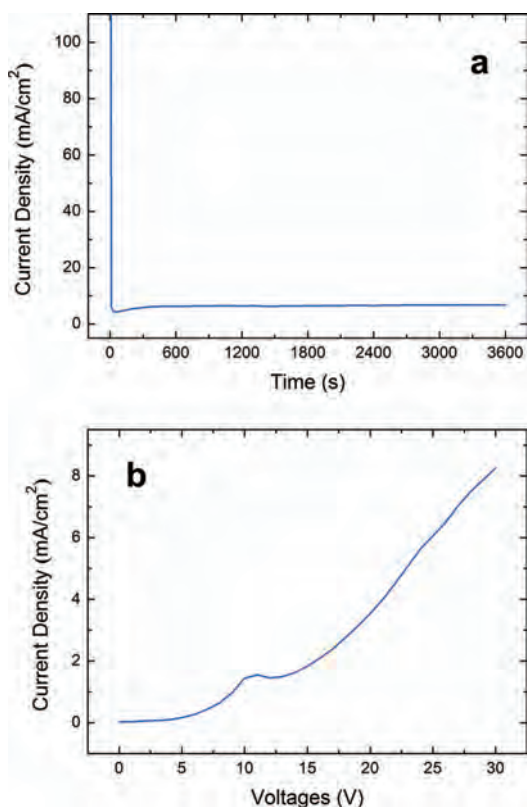


**Figure 7.** (a) *i-t* curves for titanium anodization at potentiostatic mode and (b) *E-i* curves for titanium oxide film grown at potential-sweep mode.

an assumption: for the surface of the mechanically and chemically polished titanium samples, there must be many local defects. At the initial stage of potentiostatic anodizing process, the current density is very large, especially at the defect sites. As a result, TiO<sub>2</sub>

micro-crystals are randomly emerged on the surface of titanium substrate due to very high local current density at the defect sites. Meanwhile, a layer of titanium oxides (mainly composed of TiO<sub>2</sub> and also including considerable titanium suboxides and titanium hydroxides) with plenty of absorbed water is formed in milliseconds.<sup>30</sup> Subsequently, because the crystalline oxides have a better ionic conductivity than the amorphous, the crystallized sites will act as ionic conduction channels. Therefore, TiO<sub>2</sub> crystals will nucleate and keep growing with time around these formed micro-crystals, accompanied by the conversion of titanium suboxides and hydroxides into TiO<sub>2</sub>. TiO<sub>2</sub> dominated films and “flower-like” TiO<sub>2</sub> crystalline grains will be developed when the anodic potential is high enough (Figs. 2 and 4). However, the reason why “flower-like” structure rather than other shapes of crystal are developed is still unknown. To the best of our knowledge, the OER and the breakdown around these crystals may play a key role. It should be noted that besides these well crystallized grains, the remaining part of the potentiostatically grown film, i.e. the region where has no local defects and hence no local heating generated, also shows a crystalline behavior. Thus, the crystalline structure of the less-crystallized region of the oxide film grown at potentiostatic mode may be mainly encouraged by the internal compressive stresses.<sup>18</sup>

For the potential-sweep mode, the current density is initially very small and increases with potential, the growth and crystallization of anodic titanium oxide film is a slow, continuous evolving process (Fig. 8). Hence no high local current density and then no anatase micro-crystals as found in the potentiostatic condition are generated in the beginning of the potential-sweep anodizing process. As a result, no “flower-like” crystalline grains are produced. The surface feature and crystalline behavior of the potentiodynamically grown film are relatively homogeneous (Figs. 1 and 2). Furthermore, similar to the less-crystallized part of the fast-grown film, the crystallization of the slow-grown film may be also developed by the internal compressive stresses, which is induced by the PBR and the electrostriction pressure.<sup>18,20</sup>

For the combined mode, the formed titanium oxide film shows features very close to the potential-sweep film: with smooth surface and homogeneously crystallized structure (Figs. 1 and 2). Because of the barrier layer of titanium oxide formed at the potential-sweep

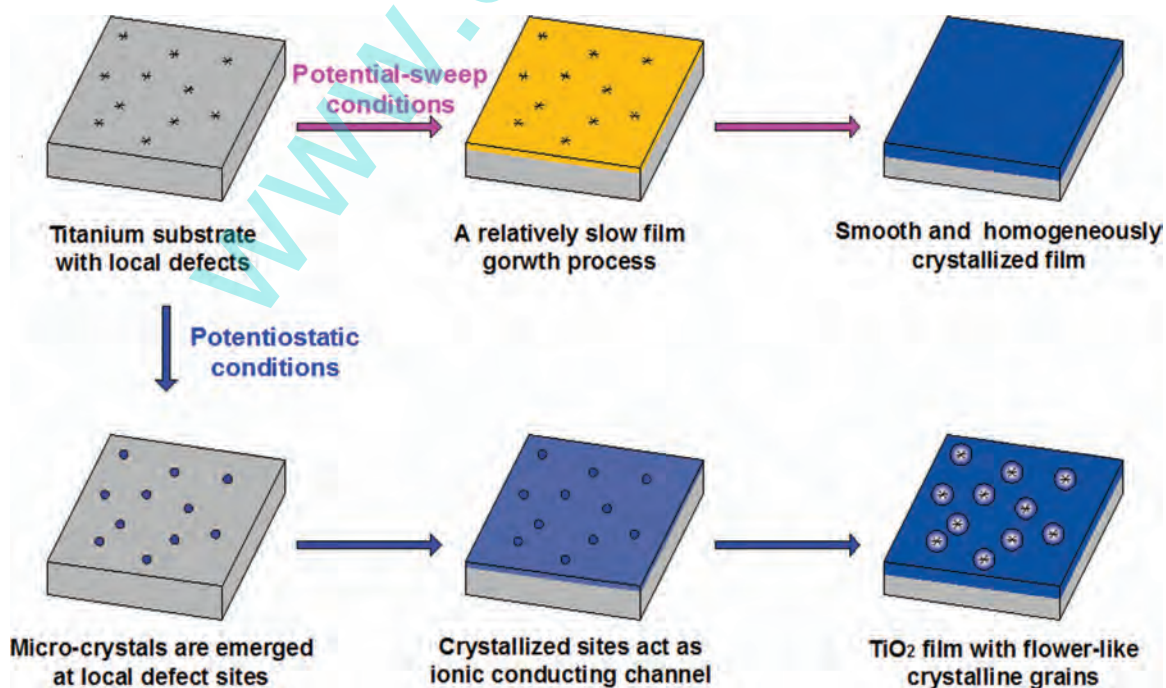


**Figure 8.** Schematic illustration of the growth and crystallization behavior of anodic titanium oxide films under potentiostatic and potential-sweep anodization modes.

stage (Table IV), there is no high local current density emerged at the beginning of the potential-aging stage, hence no “flower-like” anatase grains are generated. At the potential-aging stage, the formation and crystallization of titanium oxide film are limited by the formed barrier layer. The growth of the anodic titanium oxide film is in fact in a state of dynamic equilibrium: with the film growth rate very close to the film dissolution rate. Titanium oxide film grows mainly at the metal/oxide interface and dissolves at the oxide/solution interface. Although the overall film thickness keeps a constant value, the internal compress stresses can be generated due to the growth of titanium oxides at the metal/oxide interface. This may be why the crystallinity of the film formed at combined mode is slightly higher than that of the potentiodynamically formed film (Fig. 1a).

### Conclusions

The influence of anodization modes on the growth and crystallization behavior of titanium oxide films has been investigated by performing titanium anodization in 0.1 M H<sub>2</sub>SO<sub>4</sub> solution at potentiostatic, potential-sweep and combined modes with the same final voltage of 30 V. The conclusions of this study are listed as below:

1. It is revealed that the film formed at potentiostatic mode is rougher, thicker and more crystalline as compared to the film grown under potential-sweep and combined conditions. The XPS analysis indicates that the formed oxide films on titanium are mainly comprised of TiO<sub>2</sub>, and the slow-grown film contains a larger percent of O<sup>2-</sup> species. The EIS results show that titanium anodized film includes an outer porous layer and an inner barrier layer, and the barrier layer thickness of the potential-sweep sample is much higher than that of the potentiostatically grown film.
2. Under potentiostatic conditions, the current density is usually very large in the very beginning stage of anodizing process, especially at the local defect sites. As a result, TiO<sub>2</sub> micro-crystals are randomly emerged due to very high local current density or local heating, and “flower-like” crystalline grains will be lastly formed in anodic titanium oxide film. In the case of potential-sweep and combined modes, the formation and crystallization of anodic titanium oxide film is a relatively slow process, a layer of titanium oxide with smooth surface and homogeneously crystallized structure is formed.

### Acknowledgments

This work was supported by the program of National Natural Science Foundation of China (NSFC, No. 20976058).

### References

1. B. Bozzini, P. Carlino, L. D'urzo, V. Pepe, C. Mele, and F. Venturo, *J. Mater. Sci.: Mater. M.*, **19**, 3443 (2008).
2. M. Dubey and H. He, *Nanosci. Nanotechnol. Lett.*, **4**, 548 (2012).
3. Y. Gönüllü, G. C. M. Rodriguez, B. Saruhan, and M. Ürgen, *Sensor. Actuat. B: Chem.*, **169**, 151 (2012).
4. Y. Li, X. Lv, and J. Li, *Appl. Phys. Lett.*, **95**, 113102 (2009).
5. M. Diamanti, M. Ormellese, E. Marin, A. Lanzutti, A. Mele, and M. Pedferri, *J. Hazard. Mater.*, **186**, 2103 (2011).
6. M. S. Sikora, A. V. Rosario, E. C. Pereira, and C. O. Paiva-Santos, *Electrochim. Acta*, **56**, 3122 (2011).
7. L. Aloia Games, A. Gomez Sanchez, E. Jimenez-Pique, W. H. Schreiner, S. M. Ceré, and J. Ballarre, *Surf. Coat. Technol.*, **206**, 4791 (2012).
8. W. Simka, A. Sadkowski, M. Warczak, A. Iwaniak, G. Dercz, J. Michalska, and A. Maciej, *Electrochim. Acta*, **56**, 8962 (2011).
9. M. A. Henderson, *Surf. Sci. Rep.*, **66**, 185 (2011).
10. C. Liu, Y. Wang, M. Wang, W. Huang, and P. K. Chu, *Surf. Coat. Technol.*, **206**, 63 (2011).
11. J. L. Delplancke, A. Garnier, Y. Massiani, and R. Winand, *Electrochim. Acta*, **39**, 1281 (1994).
12. Z. Xia, H. Nanjo, T. Aizawa, M. Kanakubo, M. Fujimura, and J. Onagawa, *Surf. Sci.*, **601**, 5133 (2007).
13. P. Bourdet, F. Vacandio, L. Argeme, S. Rossi, and Y. Massiani, *Thin Solid Films*, **483**, 205 (2005).
14. S. Kudelka, A. Michaelis, and J. Schultze, *Electrochim. Acta*, **41**, 863 (1996).
15. D. Wiesler and C. Majkrzak, *Physica B: Condensed Matter*, **198**, 181 (1994).
16. J. Yahalom and J. Zahavi, *Electrochim. Acta*, **15**, 1429 (1970).
17. J. Yahalom and J. Zahavi, *Electrochim. Acta*, **16**, 603 (1971).
18. J. Leach and B. Pearson, *Corros. Sci.*, **28**, 43 (1988).
19. J. Vanhumbecck, L. Ryelandt, and J. Proost, *Electrochim. Acta*, **54**, 3330 (2009).
20. T. Shibata and Y. Zhu, *Corros. Sci.*, **37**, 253 (1995).
21. T. Shibata and Y. Zhu, *Corros. Sci.*, **37**, 133 (1995).
22. C. Dyer and J. Leach, *J. Electrochem. Soc.*, **125**, 1032 (1978).
23. H. Habazaki, M. Uozumi, H. Konno, K. Shimizu, P. Skeldon, and G. Thompson, *Corros. Sci.*, **45**, 2063 (2003).
24. D. Capek, M. Gigandet, M. Masmoudi, M. Wery, and O. Banakh, *Surf. Coat. Technol.*, **202**, 1379 (2008).
25. J. Vanhumbecck, H. Tian, D. Schryvers, and J. Proost, *Corros. Sci.*, **53**, 1269 (2011).
26. J. Nelson and R. Oriani, *Corros. Sci.*, **34**, 307 (1993).
27. N. Sato, *Electrochim. Acta*, **16**, 1683 (1971).
28. A. Prusi, L. Arsov, B. Haran, and B. Popov, *J. Electrochem. Soc.*, **149**, 491 (2002).
29. S. A. Fadl-allah and Q. Mohsen, *Appl. Surf. Sci.*, **256**, 5849 (2010).
30. Z. Xia, H. Nanjo, H. Tetsuka, T. Ebina, M. Izumisawa, M. Fujimura, and J. Onagawa, *Electrochem. Commun.*, **9**, 850 (2007).
31. Y. Leprince-Wang, *Surf. Coat. Technol.*, **150**, 257 (2002).
32. T. Ohtsuka and T. Otsuki, *Corros. Sci.*, **45**, 1793 (2003).
33. D. D. Macdonald, *J. Electrochem. Soc.*, **139**, 3434 (1992).
34. M. E. P. Souza, M. Ballester, and C. M. A. Freire, *Surf. Coat. Technol.*, **201**, 7775 (2007).
35. C. H. Hsu and F. Mansfeld, *Corrosion*, **57**, 747 (2001).